



## Olive fruit ripening characterisation based on electrical capacitance measurements

Daniel Argüello, Miguel Noguera, Andrés Mejías, Juan Manuel Enrique, Arturo Aquino\*

Centro de Investigación en Tecnología, Energía y Sostenibilidad, Universidad de Huelva, Carretera Huelva-Palos, S/N, 21810, Palos de la Frontera, Spain

### ARTICLE INFO

#### Keywords:

Olive fruit ripening  
Electrical capacitance  
Olive fat content  
Intra-sample variability  
Electrical modelling

### ABSTRACT

Olive fruit ripening involves the accumulation of fat content through lipogenesis. The completion of this complex process is considered a reliable indicator of the optimal time for harvesting. While chemical and magnetic resonance analyses, among other, can accurately determine fat content, these methods are costly and require specialized personnel, making them impractical for large-scale testing. Alternatively, visual grading methods are widely used, although recent studies have shown that the external appearance of fruits may not always reliably indicate ripeness. This paper investigates the influence of olive fruit maturation on their electrical behaviour, specifically on their ability to store electrical charge. To this end, a low-cost and portable field meter capable of measuring the electrical capacitance of olive fruits was designed and developed. Subsequently, 110 olive samples were measured weekly from September to harvest time in November. These samples were also subjected to chemical analysis for reference. The analysis of this data revealed high intra-sample variability, consistent with recent studies. Notably, strong correlations of up to 0,9741 emerged between capacitance measurements and gold-standard fat content on dry matter values after accounting for intra-sample variability. In this case, a Root-Mean-Square-Error value of 2,66% was calculated when using the regression line to estimate fat content on dry matter from capacitance values. Furthermore, no significant differences were observed between the distributions of the reference values and the estimated values. These findings pave the way for the development of an affordable tool to accurately assess the ripening stage directly in the field, and to expand our understanding about the ripening process.

### 1. Introduction

The olive crop (*Olea europaea* L.) and its associated market constitute an exceptional economic engine for the countries in the Mediterranean basin. The EU accounts for approximately 70% of global olive oil production, with Spain and Italy contributing around 80% of that total [1]. Besides its economic value, olive oil, the primary by-product of the olive sector, is increasingly regarded by consumers as a vital ingredient for a healthy diet due to its richness in valuable nutrients and bioactive compounds with therapeutic benefits [2]. These features place olive oil as the cornerstone of the Mediterranean diet, declared Intangible Cultural Heritage of Humanity by UNESCO in 2010 [3].

Traditionally, the olive sector has been characterised by a limited penetration of technological support. The traditional olive orchard is defined by wide cultivation patterns (8×8 m between trees (100–300 trees/ha)). Under these conditions, the crop can maintain production in

rain-fed conditions. However, the search for increasing profitability of olive farms has conducted to new cultivation paradigms, being the main current trend the super high density (SHD) olive orchard. The main feature of this cultivation system is its compact cultivation pattern, which consists of rectangular layouts with spacing of 1–1,5 m within rows and 3–3,5 m between rows. Under these conditions, plant density exceeds 1500 trees/ha, which maximises the productivity per land surface [4]. Furthermore, the trees are trained to build continuous hedgerows, thus resulting in a regular two-dimensional tree shape that eases mechanisation of management labours such as pruning, harvesting, or phytosanitary control [5]. These features expand the profitability of SHD olive orchards when comparing to previous cultivation systems, which suggests their probable preponderance in the future. SHD olive orchards are nowadays supported by standard cultivation protocols which facilitate their management, although there are still pending aspect susceptible of outstanding improvement. In this sense, precision

\* Corresponding author.

E-mail addresses: [daniel.arguello@alu.uhu.es](mailto:daniel.arguello@alu.uhu.es) (D. Argüello), [miguel.noguera@diesia.uhu.es](mailto:miguel.noguera@diesia.uhu.es) (M. Noguera), [mjias@diesia.uhu.es](mailto:mjias@diesia.uhu.es) (A. Mejías), [juanm.enrique@diesia.uhu.es](mailto:juanm.enrique@diesia.uhu.es) (J.M. Enrique), [arturo.aquino@diesia.uhu.es](mailto:arturo.aquino@diesia.uhu.es) (A. Aquino).

<https://doi.org/10.1016/j.atech.2024.100696>

Received 14 November 2024; Received in revised form 2 December 2024; Accepted 2 December 2024

2772-3755/© 2024 The Author(s). Published by Elsevier B.V. This is an open access article under the CC BY license (<http://creativecommons.org/licenses/by/4.0/>).

farming strategies are gaining interest among the research community and industry.

Precision farming is a management approach designed to assess spatial and temporal variability within an agroecosystem, and to apply location-specific treatments using a variety of technologies and methods [6]. Crop variability is influenced by spatial and temporal diversity in factors such as soil quality, incidence of plant diseases, exposure to solar radiation or water sources, climate conditions, etc. Precision farming customises crop management to crop variability by applying agronomic inputs and by implementing management practices at variable rates to meet the specific needs of different zones within the field. This translates into cost savings and minimised environmental impact. One key area of focus for precision farming in the context of oliviculture is the monitoring of the olive fruit ripening process.

Olive ripening involves the chemical and physical changes that make olive fruits edible. This is the result of a complex combination of physiological and biochemical pathways, with a high genetic component, which are also influenced by climatic and culture conditions. One of the most relevant chemical changes used as ripening indicator is the accumulation of fat content, process known as lipogenesis. Lipogenesis presents a variation that conforms to a sigmoid-type curve established because of three different stages. The first phase (slow biosynthesis) occurs in newly formed fruits and culminates with the stone hardens. The second phase (accelerated biosynthesis) takes place after stone hardening and lasts until the change of pigmentation of the fruit from green to yellowish-green. The third (stationary) phase consists of a progressive decrease in the rate of oil formation, which eventually ceases, thus signifying the end of lipogenesis [4]. The characteristics that are intended to be attributed to the oil determine the optimum point of maturation, however the completion of lipogenesis is considered as an indicator of the optimum time for harvesting [7].

Traditionally, the fat content of olives has been determined using chemical methods such as Soxhlet extraction [8] or nuclear magnetic resonance [9]. These techniques are costly and require specialised laboratory equipment and skilled personnel. Consequently, their application for monitoring olive ripening with high spatio-temporal resolution is limited. As a result, olive growers typically rely on subjective methods, such as visual assessment of fruit colour, to determine ripeness. However, recent studies suggest that internal quality parameters may vary independently of the fruit's external appearance, indicating that colour may not be the most reliable indicator of ripeness [10]. On the other hand, lipogenesis is influenced by climatic and culture conditions, resulting in variable ripening rates across the olive grove. Since management practices can partially offset this variability, precise monitoring of fat content would enable site-specific interventions to address heterogeneity during ripening. Furthermore, this data-driven approach would empower growers to make informed harvest decisions based on objective criteria, thus facilitating the development of diversified production strategies aligned with precision agriculture principles. Furthermore, instrumental research in fruit quality assessment can benefit other stakeholders in the olive sector, such as processors, distributors and handlers.

Implementing a precision farming approach to ripening control requires developing new tools capable of accurately monitoring ripening parameters in both space and time. In recent decades, the research community has proposed various alternatives to traditional chemical methods for fruit quality assessment. These include several technologies, such as image processing based on visual features [11], multispectral imaging [12], hyperspectral imaging [13], electronic nose devices [14], ultrasonic-based methods [15], and electrical properties-based methods [16].

This work falls into the category of methods based on electrical properties, as it presents a methodology to assess the fat content of olive fruits based on their electrical behaviour. The relationship between electrical variables and quality parameters of fruits is a relatively mature topic [17–19]. Techniques based on the electrical properties of fruits and

vegetables have attracted widespread attention due to the simplicity and speed of the method, as well as its high sensitivity to fruit and vegetable quality parameters. Changes in electrical characteristics can infer interior quality changes indirectly. In this regard, electrical properties have been demonstrated to have a relationship with quality indicators of multiple crops (nectarines [20], persimmon [21], tomato [22], garlic [23], mango [24], pitahaya [25], mangosteen [26], pears [27], date palm [28], etc). However, research focused on olive fruits is scarcer. Recent studies have observed that the conductivity of olive fruits increases according to the stage of ripeness, at different rates depending on the olive variety [29]. This highlights electrical conductivity as a potential indicator of the optimal harvesting time. Nevertheless, a non-negligible capacitance component can be inferred from this study, which is yet to be addressed. Furthermore, the interaction between conductivity and moisture was not explored by the authors, even though it is a priori plausible to consider this interaction strong.

The present study aims to advance the state of the art regarding the influence of olive maturation on its electrical behaviour. Specifically, this work assesses the correlation between olive capacitance and a widely accepted ripening indicator, such as fat content. Capacitance measures a capacitor's ability to store electric charge, and the presence of a dielectric material between capacitor plates enhances this ability, thus increasing capacitance [16]. The initial hypothesis is that the fat accumulated by olives during maturation acts as a dielectric, affecting their ability to store electric charge and thereby affecting capacitance. To test this hypothesis, a custom-built LCR meter was developed, specially designed to operate under field conditions. This prototype was used to periodically characterize the capacitance of olive fruit samples throughout a full ripening campaign. The relationship between capacitance and gold-standard fat content values was then analysed to evaluate the potential of capacitance as a reliable indicator of fat content.

## 2. Materials and methods

### 2.1. Study site description

The study site was a commercial olive orchard (*Olea europaea* L., cv. Picual) managed by Nuestra Señora de la Oliva, S.C.A., located in the province of Huelva, Andalusia, Spain (37°20'28,96" N and 7°01'54,98" O). This orchard follows a traditional planting layout with a spacing pattern of 7×7 m. Although the farm spans over 200 ha, a one-hectare plot was delineated for this experiment to ensure uniform ripening conditions within the study area. The climate at the experimental site is classified as Csa (hot-summer Mediterranean) according to the Köppen-Geiger classification [30], with an average annual rainfall of approximately 600 mm concentrated between October and May. This seasonal pattern leads to a pronounced drought period during spring and summer, which coincides with demanding phenological processes for the plants (inflorescences/flowering/fruit set, fruit growth and fat accumulation). To mitigate water stress during this period, the experimental plot is equipped with a drip irrigation system.

### 2.2. Experimental field protocol design

To test the initial hypothesis presented in this research, it was essential to gather a comprehensive dataset of capacitance measurements from olives across a broad spectrum of maturation stages, along with their corresponding reference values for fat content obtained through standard chemical methods. To obtain this dataset, periodic sample collections were conducted that spanned the entire ripening process of olive fruits. The initial sample collection occurred after the post-summer fruit growth phase in September and was repeated weekly until harvest in November, resulting in a total of 110 olive samples collected in six sampling events. Each sample unit consisted of approximately 200 g of olives collected from a randomly selected tree. The olives belonging to each sample were selected to have the same external

appearance as an indicator of maturity, thus following the classic approach [31]; the location of fruits within the tree, or any other factor, was not taken into account.

### 2.3. Olive fruit capacitance measurement protocol

Immediately after picking, the olive samples were packaged, labelled, and refrigerated for transport to the laboratory. Once at the laboratory, capacitance measurements were performed according to the following protocol. Samples were kept refrigerated to maintain a consistent temperature and were removed from the refrigerator just before measurement. From each 200 g sample, 15 olives were randomly selected for subsampling. Capacitance of each olive was individually measured using the device described in Section 2.5. The process involved inserting the device's metallic probe through the olive epicarp at a predetermined position (centred along the fruit's minor axis) until it reached the mesocarp. The capacitance measure was then saved on the device's SD card, and the olive was removed. Between measurements, the metallic probe was cleaned with paper, and the device was recalibrated. After measuring the 15 olives for each sample, they were repackaged with the rest of the sample and refrigerated. All samples collected in a single sampling event were measured the same morning they were picked, followed by standard chemical analysis to obtain reference fat content values.

### 2.4. Gold-standard fat content determination

The reference analysis of fat content was conducted in the laboratory following official methodologies. Fat content was determined in two forms: fat content per dry matter (FCDM) and fat content per fresh weight (FCFW).

First, the sample moisture ( $M$ ) was determined using the oven-drying method at 105 °C [32]. According to this procedure, a 25 g portion of the sample is placed in a porcelain capsule and dried at 105 °C for 6 hours. After drying, the sample is cooled in a desiccator, weighed, and returned to the oven, repeating these steps until the difference in weight between two consecutive measurements is less than 0,02 g. At this point, the difference between the initial and final weight is taken as the sample's moisture content,  $M$ .

The reference analysis of FCFW was performed using the Soxhlet method [8]. This method involves placing the dried sample (used for moisture determination) in a Soxhlet extractor, where fat is extracted by exposing the sample to n-hexane for 4 hours. The sample is then returned to the oven at 105 °C to remove any solvent residues. The amount of fat extracted is used to determine FCFW, and from this value, FCDM is calculated using the following equation:

$$FCDM = \frac{FCFW}{100 - M} \quad (1)$$

### 2.5. Design and implementation of a field meter prototype for measuring olive fruit capacitance

#### 2.5.1. Field meter design and implementation

To measure the capacitance of olive samples, a portable, low-power meter was designed using the Arduino Capacitor library [33]. The components used in the developed meter are commercially available and easily replaceable, ensuring straightforward maintenance in case of eventual degradation and supporting long-term usability. Given that device size is a key factor for ease of handling, the meter was built around an Arduino MKR Zero board [34], which incorporates a low-power SAMD21 Cortex M0+ 32-bit microcontroller. This microcontroller board was chosen for its efficient and versatile features, which make it ideal for this application. It provides strong processing capabilities while maintaining a low power profile, crucial for prolonged use in the field. Additionally, it supports lithium battery power, ensuring

portability and convenience, and includes an onboard regulated charger for straightforward recharging without the need for external circuitry. The board also integrates a microSD card interface, enabling it to store data efficiently, which is essential for applications requiring continuous data logging or large data storage capacity. The mentioned Arduino Capacitor library [33] was modified to work with this specific microcontroller, as its architecture is not directly compatible.

The meter was designed with the following key features:

- Efficient field measurement, enabling ease of use in on-site conditions.
- Storage of measurement data in CSV format, allowing for streamlined processing on a computer.
- Organized data storage, with files clearly labelled by measurement area within the plantation to facilitate easy identification.
- Visual feedback via a low-power OLED display, showing essential information such as the name of the active data file, the count of measurements taken, the current reading, battery status, and microSD card availability.

All of these features were integrated into the custom software developed specifically for this meter. Fig. 1 provides an overview of the meter's general block diagram. The interface design includes three push buttons (DATA, FILE, and RESET), which enable the execution of each function, ensuring ease and efficiency in use. As illustrated in Fig. 1, the meter is powered by a 3,7 V lithium-ion battery, providing sufficient field autonomy for prolonged operation. Additionally, the battery can be conveniently recharged on-site with a portable power bank, enhancing its usability in remote conditions.

The developed meter, shown in Fig. 2, features a data acquisition button (DATA), a file selection button (FILE), and a sample measurement reset button, which does not affect previous measurements. It is equipped with two fixed conductive plates, spaced 2,54 mm apart, located at the top (see Fig. 2). When the olive is pierced by these plates, the olive itself acts as the dielectric for the capacitor. The insertion depth of the conductive plates into the olive is naturally limited by both the size of the olive and a stop provided by the meter's support. This ensures that the mesocarp between the plates remains as consistent as possible when piercing the olive.

#### 2.5.2. Field meter calibration

The meter was calibrated by comparing its experimental results with those obtained from a precision capacitance meter (ESR Multi PKT-2155), which served as the reference. Identical conductive plates were used in both meters to ensure consistency during the calibration process.

The Capacitor library measures capacitance between two of its analogue pins, with a simplified circuit diagram for the measurement shown in Fig. 3. The diagram illustrates the capacitance to be measured ( $C_m$ ), along with pin A2, which provides a 3,3-volt voltage, and pin A3, which is used for the measurement. Additionally, an intrinsic capacitance ( $C_{sc}$ ), representing stray capacitance specific to each board, can be modelled. The value of this capacitance must be determined and entered as a parameter in the library to ensure proper calibration of the meter.

To calibrate the developed meter, a reference non-electrolytic 1  $\mu$ F capacitor was first measured using the precision capacitance meter, yielding a value of 1.021  $\mu$ F. The same capacitor was then measured with the developed meter, which provided a reading of 1,03  $\mu$ F. By initially setting the stray capacitance in the meter's control software to 20 pF and using these measurements, the necessary stray capacitance value necessary for accurate calibration can be calculated as:

$$C_{sc} = \frac{C_m(V_{ref} - V_m)}{V_m} = \frac{102,1(1.023 - 895)}{895} = 14,6 \text{ pF} \quad (2)$$

where 1.023 is the maximum ADC converter value on the board.

To verify the meter's accuracy, several capacitors were measured

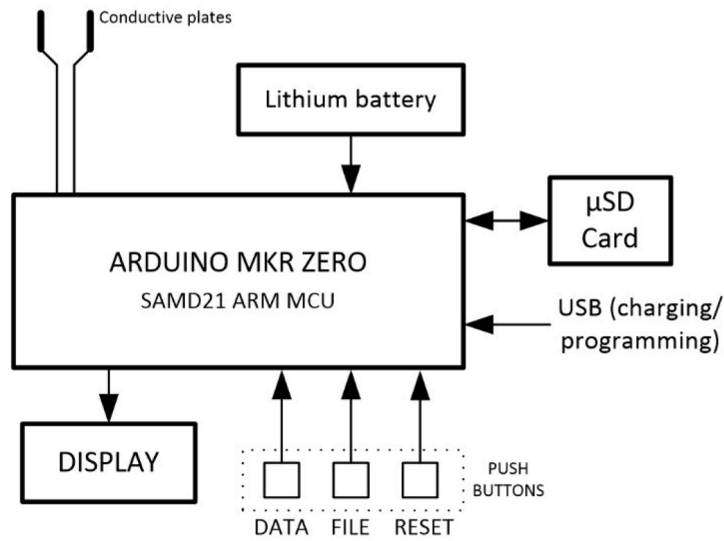


Fig. 1. Field meter's block diagram.



(a)



(b)

Fig. 2. Field meter designed to measure the electrical capacitance of intact olive fruits: (a) external view of the developed field meter; (b) demonstration of the capacitance field meter in use for measuring the electrical capacitance of an olive fruit.

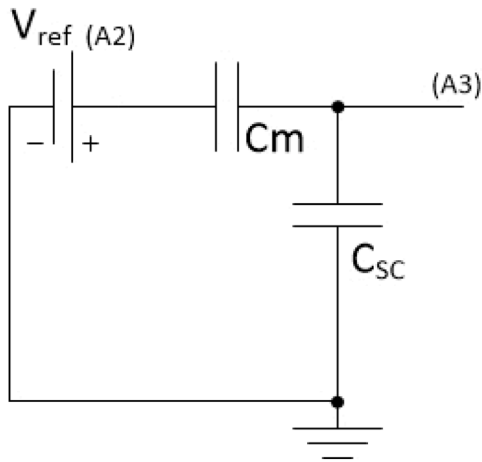


Fig. 3. Electrical model of the microcontroller’s analogue pins used for capacitance measurement.

Table 1

Experimental results assessing the accuracy of the developed meter in comparison to a precision capacitor for measuring capacitors with known capacitance values.

Nominal Value (pF)	Measured Value (Precision capacitor) (pF)	Measured Value (Developed meter) (pF)	Relative Error (%)
100	101,2	102,0	0,8
220	218,5	224,2	2,6
470	472,8	459,1	2,9
1.000	1.003,5	1.030,0	2,6
2.200	2.197,8	2.140,6	2,6
4.700	4.692,4	4.606,3	1,8
10.000	10.025,5	9.790,0	2,3
22.000	21.956,8	21.356,0	2,7
47.000	47.078,1	45.590,0	3,2
100.000	99.921,3	97.990,0	1,9

once the correct stray capacitance was set. The measurements obtained with the developed meter were compared to those recorded using a precision capacitor (ESR Multi PKT-2155). Table 1 presents the relative error for various measurements taken with the field meter in comparison to the precision capacitor, considered as providing the true values of the capacitors used as test elements. The results show that relative errors ranged from 0,8% to 3,2%, demonstrating the device’s accuracy and reliability within these limits. This level of performance makes the device well-suited for the requirements of this study.

2.6. Methodology for evaluating the formulated hypothesis

This section describes the methodology followed to evaluate the hypothesis formulated in this study, which posits that olive ripening influences the fruit’s ability to store electrical charge.

As it was previously described, 110 groups of 200 g of olive fruits were gathered for this study. Then, the following numerical set was assigned to every group:

$$FS_i = \{F_i, \overline{FCFW}_i, \overline{FCDM}_i \mid i = 1 \dots 110\} \tag{3}$$

where, for the *i*-th set, *F<sub>i</sub>* is the set of 15 capacitance values in farad units (F) measured from 15 olive fruits randomly selected,  $\overline{FCFW}_i$  and  $\overline{FCDM}_i$  are the fat content per fresh weight and per dry matter, respectively, both expressed as percentage (%) and determined by chemically analysing the corresponding whole *i*-th group of 200 g of olive past. Thus,  $FCFW_i(\overline{FCFW}_i, \sigma_{FCFW_i})$  and  $FCDM_i(\overline{FCDM}_i, \sigma_{FCDM_i})$  can be seen as two *i*-th statistical populations of fat content values with known average and

unknown individuals and standard deviation, and  $F_i(\overline{F}_i, \sigma_{C_i})$  is a random sample of an unknown population of electrical capacitance measures;  $F_i(\overline{F}_i, \sigma_{C_i})$  represents the population with 15 individuals, their average and standard deviation. For each sample *F<sub>i</sub>*, measurements falling outside the range  $\overline{F}_i \pm 2\sigma_{C_i}$  were identified and removed as outliers. To assess whether the electrical capacitance mathematically explains the fat content of olive fruits,  $\overline{F}_i$  values were contrasted against those of  $\overline{FCFW}_i$  and  $\overline{FCDM}_i$  employing linear regression analysis, and the Pearson’s coefficient of determination, *R*<sup>2</sup>, was calculated for both cases. The obtained regression lines,  $r_{FCFW}(\overline{F}_i)$  and  $r_{FCDM}(\overline{F}_i)$ , were then used to derive the sets of estimated fat content values  $\{FCFW'_i\}$  and  $\{FCDM'_i\}$ , respectively. Next, the Root-Mean-Square-Error (RMSE) relative to the mean and given as percentage,  $RMSE_{mean}^{FCFW}$  and  $RMSE_{mean}^{FCDM}$ , was calculated for both cases as follows:

$$RMSE_{mean}^{FCFW} = \frac{\sqrt{\frac{1}{n} \sum_{i=1}^n (\overline{FCFW}'_i - \overline{FCFW}_i)^2}}{\sum_{i=1}^n \overline{FCFW}_i} \cdot 100, \tag{4}$$

$$RMSE_{mean}^{FCDM} = \frac{\sqrt{\frac{1}{n} \sum_{i=1}^n (\overline{FCDM}'_i - \overline{FCDM}_i)^2}}{\sum_{i=1}^n \overline{FCDM}_i} \cdot 100$$

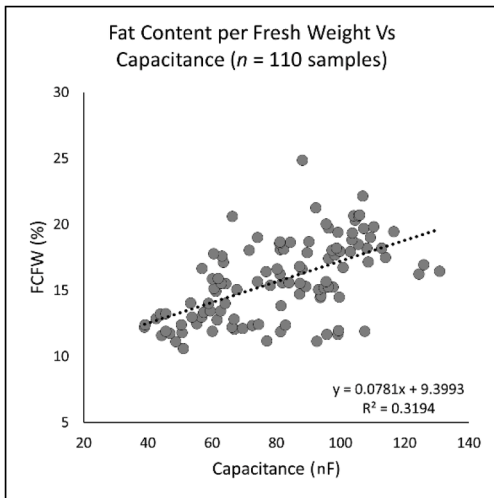
Finally, the distributions of fat content references  $\overline{FCFW}_i$  and  $\overline{FCDM}_i$  were compared to their corresponding derived distributions of  $\overline{FCFW}'_i$  and  $\overline{FCDM}'_i$  values, to assess their similarity. To this end, a T-test for comparing the means of the distributions [35], incorporating Levene’s test for equality of variances [36], was conducted at a significance level of *p* < 0,05 with a 95% confidence interval.

3. Results and discussion

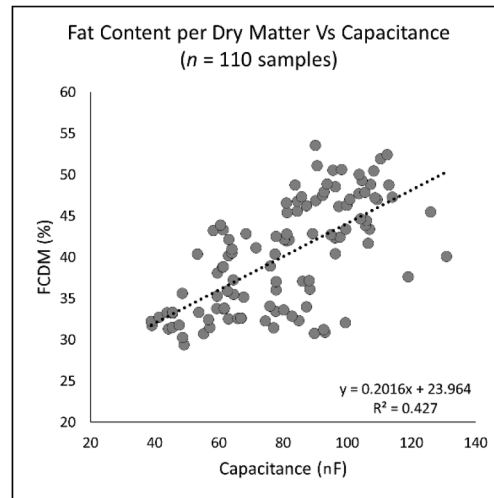
Fig. 4 – (a-1) and (b-1) shows the correlation obtained by facing the average electrical capacitance values for the 110 sets,  $\overline{F}_i$ , with the corresponding fat content reference values  $\overline{FCFW}_i$  and  $\overline{FCDM}_i$ . As it can be observed, a certain linear trend can be observed from the clouds of points, although yielding modest *R*<sup>2</sup> values, or even poor in the case of *FCFW*. In this context, the first inclination might be to refuse the hypothesis formulated in this paper, but further analysis revealed rich and interesting results, which advocates for the contrary conclusion.

First, despite the previous findings, let’s explore the hypothesis that electrical capacitance closely correlates with the fat content in olive fruits. If this holds, the modest correlation values observed could be due to the random sampling of 15 capacitance values per fruit set, *F<sub>i</sub>*, gives as result average values,  $\overline{F}_i$ , poorly representing the whole unknown populations of electrical capacitance values. This poor representativity would be attributed to a non-negligible intra-population variability, which the maturity index formulated by Ferreira et al. [31] is not capable to discern. Due to the lack of methods to evaluate the fat content on single olive fruits, the bibliography is sparse in the characterisation of the fat content variability for olives having the same maturity index, although a recent study supports the inaccuracy of this indicator. Indeed, Grilo et al. [10] conducted an experiment to evaluate the influence of the position of olive fruits (in the upper and lower layers) within the tree on several features. In light of the analysed results, they concluded that the environmental conditions determined by fruit position in the canopy (e.g. temperature, light, etc.) were the major factors influencing oil accumulation. Furthermore, they also found that differences in fat content between fruits from different zones of the tree were independent of their external appearance, suggesting that the maturity index may not be a reliable indicator of ripeness in the end.

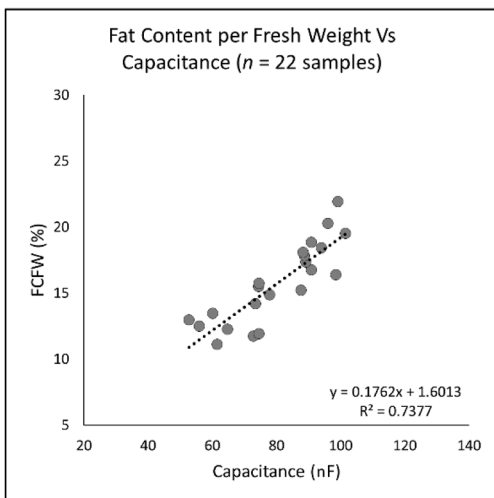
To evaluate the validity of this hypothesis, further analysis was conducted with the aim of virtually increasing the number of fruits



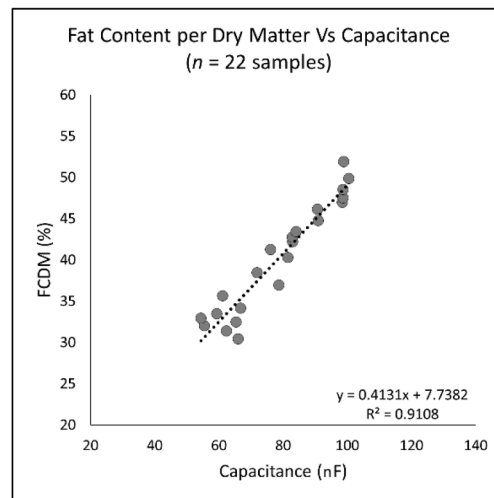
(a-1)



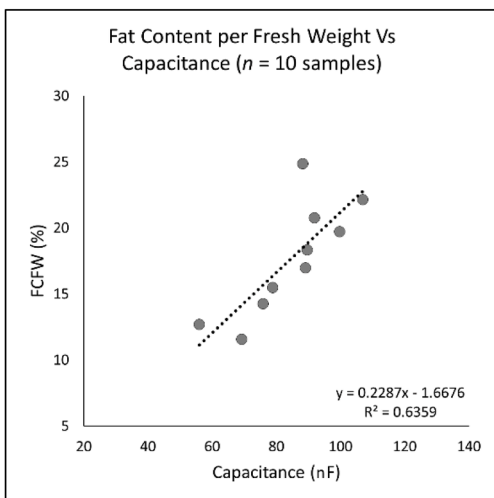
(b-1)



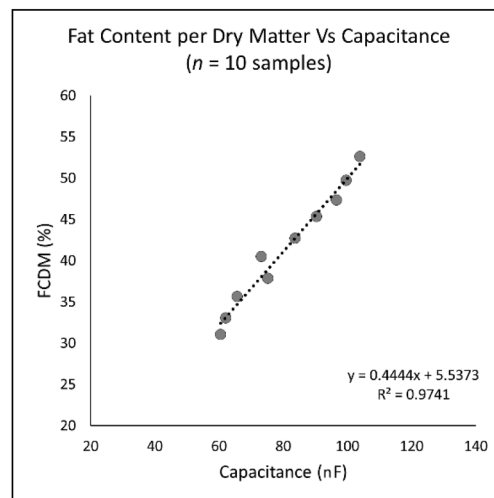
(a-2)



(b-2)



(a-3)



(b-3)

(caption on next page)

**Fig. 4.** Correlation study between the different sets of fat content per fresh weight (FCFW) and per dry matter (FCDM) values, and the average capacitance measures in farad units (F) of olive samples: (a-1) and (b-1) correlation study between the fat content reference values  $\overline{FCFW}_i$  and  $\overline{FCDM}_i$ , chemically determined from the 110 original sets,  $\overline{F}_i$ , and the average capacitance values measured from the 15 olive fruits randomly selected for every set; (a-2) and (b-2) correlation study between the average fat content reference values  $\overline{FCFW}_{i,22}$  and  $\overline{FCDM}_{i,22}$ , calculated from the 22 clustered fruit sets,  $\overline{F}_{i,22}$ , and the average capacitance values measured from the 75 olive fruits samples belonging to every clustered set; (a-3) and (b-3) correlation study between the average fat content reference values  $\overline{FCFW}_{i,10}$  and  $\overline{FCDM}_{i,10}$ , calculated from the 10 fruit sets clustered based on fat content percentiles,  $\overline{F}_{i,10}$ , and the average capacitance values measured from the olive fruits samples belonging to every clustered set.

sampled per statistical population. To do so, the 110 fruit sets,  $FS_i$ , were grouped into 22 clusters, resulting the clusters from joining those sets having the closest  $\overline{FCFW}_i$  values; the same operation was performed taking  $\overline{FCDM}_i$  values as clustering criterium. Mathematically, the cluster build for FCFW is defined as:

$$C_{i,FCFW} = \{F_j, \overline{FCFW}_j \mid i = 1, \dots, 22, j \in \{1, \dots, 110\}, |C_{i,FCFW}| = 5\} \quad (5)$$

fulfilling

$$C_{i,FCFW} \cap C_{k,FCFW} = \emptyset \wedge \nexists \overline{FCFW}_l \in C_{k,FCFW} \mid \overline{FCFW}_l < \overline{FCFW}_j \quad (6)$$

Analogously, the clusters for FCDM are defined as:

$$C_{i,FCDM} = \{F_j, \overline{FCDM}_j \mid i = 1, \dots, 22, j \in \{1, \dots, 110\}, |C_{i,FCDM}| = 5\} \quad (7)$$

such as

$$C_{i,FCDM} \cap C_{k,FCDM} = \emptyset \wedge \nexists \overline{FCDM}_l \in C_{k,FCDM} \mid \overline{FCDM}_l < \overline{FCDM}_j \quad (8)$$

Finally, for both the FCFW and FCDM cases, a new fruit set of 22 instances was derived from the clusters by taking, for every cluster, the union of the five  $F_j$  sets of 15 capacitance measures each, and the average of the corresponding five fat content values:

$$\begin{aligned} FS_{i,22}^{FCFW} &= \{F_{i,22}, \overline{FCFW}_{i,22} \mid i = 1 \dots 22\}, \\ FS_{i,22}^{FCDM} &= \{F_{i,22}, \overline{FCDM}_{i,22} \mid i = 1 \dots 22\} \end{aligned} \quad (9)$$

where

$$F_{i,22} = \cup \{F_j\}, \overline{FCFW}_{i,22} = \sum \frac{\overline{FCFW}_j}{5}, \overline{FCDM}_{i,22} = \sum \frac{\overline{FCDM}_j}{5} \quad (10)$$

fulfilling

$$F_j, \overline{FCFW}_j \in C_{i,FCFW} \wedge F_j, \overline{FCDM}_j \in C_{i,FCDM} \quad (11)$$

Note that, in practice, the derived fruit sets,  $FS_{i,22}^{FCFW}$  and  $FS_{i,22}^{FCDM}$ , are effectively equivalent to what would have resulted from forming 22 groups of 1.000 g of olive fruits each, measuring the electrical capacitance of 75 randomly selected olives per group, and performing chemical analyses of FCFW and FCDM on the entire 1.000 g of olive past within each group. Analogously, two additional derived fruit sets were created,  $FS_{i,10}^{FCFW}$  and  $FS_{i,10}^{FCDM}$ , by clustering according to the percentiles of FCFW and FCDM values, respectively. Relevant information about the derived fruit sets can be found in Tables 2 and 3.

Fig. 4 – (a-2) and (b-2) graphically illustrates the correlation between the average electrical capacitance values for the derived 22 fruit sets,  $\overline{F}_{i,22}$ , and the corresponding fat content reference values  $\overline{FCFW}_{i,22}$  and  $\overline{FCDM}_{i,22}$ , respectively. Both results support validation of the formulated hypothesis, as correlation values increase to 0,7377 for the case of FCFW and to 0,9108 for FCDM, what indicates that electrical capacitance accounts for over 73% and 91% of the statistical variance in the respective variables. As in the initial case, a lower correlation was found with FCFW, which is to be expected. Indeed, contrary to FCDM, this metric provides the percentage of fat content present in the intact fruit past, thus including water content. It is well established that fruit water content can fluctuate significantly throughout the ripening process,

**Table 2**

Statistical characterisation of fruit sets  $FS_{i,22}^{FCFW}$  and  $FS_{i,22}^{FCDM}$ , derived by clustering the original set of 110 olive fruit groups of 200 g into 22 clusters. Each cluster consists of the five closest values for fat content per fresh weight, FCFW, and per dry matter, FCDM. The ranges of FCFW and FCDM values, along with the average used to represent each cluster, are provided.

	$FS_{i,22}^{FCFW} (n = 22)$		$FS_{i,22}^{FCDM} (n = 22)$	
	Interval (% of FCFW)	Average (% of FCFW)	Interval (% of FCDM)	Average (% of FCDM)
1	[10,59–11,58]	11,11	[29,36–30,89]	30,39
2	[11,64–11,86]	11,73	[31,22–31,46]	31,38
3	[11,88–12,04]	11,92	[31,70–32,26]	32,0
4	[12,10–12,35]	12,24	[32,31–32,60]	32,48
5	[12,38–12,76]	12,48	[32,60–33,25]	32,92
6	[12,79–13,20]	12,95	[33,29–33,67]	33,46
7	[13,23–13,82]	13,45	[33,75–35,13]	34,15
8	[13,99–14,48]	14,19	[35,28–36,02]	35,65
9	[14,57–15,05]	14,86	[36,09–37,24]	36,92
10	[15,12–15,29]	15,21	[37,61–38,90]	38,44
11	[15,37–15,57]	15,49	[40,07–40,41]	40,27
12	[15,57–15,88]	15,72	[40,49–41,97]	41,24
13	[16,21–16,59]	16,37	[42,07–42,40]	42,22
14	[16,61–16,94]	16,74	[42,49–42,85]	42,74
15	[17,10–17,57]	17,33	[43,22–43,82]	43,42
16	[17,66–17,94]	17,82	[43,87–45,45]	44,76
17	[18,03–18,17]	18,08	[45,55–45,56]	46,14
18	[18,19–18,62]	18,41	[46,75–47,20]	46,97
19	[18,65–19,0]	18,83	[47,27–47,84]	47,52
20	[19,34–19,69]	19,50	[47,87–48,80]	48,53
21	[19,81–20,63]	20,26	[48,85–50,53]	49,82
22	[20,64–24,85]	21,91	[50,59–53,52]	51,90

**Table 3**

Statistical characterisation of fruit sets  $FS_{i,10}^{FCFW}$  and  $FS_{i,10}^{FCDM}$ , derived by clustering the original set of 110 olive fruit groups of 200 g according to the percentiles of fat content per fresh weight and per dry matter, FCFW and FCDM, respectively. The intervals of FCFW and FCDM values, and the average taken to represent each cluster, are given.

	$FS_{i,10}^{FCFW} (n = 10)$		$FS_{i,10}^{FCDM} (n = 10)$	
	Interval (% of FCFW)	Average (% of FCFW)	Interval (% of FCDM)	Average (% of FCDM)
1	[10,59–11,93]	11,56	[29,36–31,76]	31,02
2	[12,04–13,44]	12,69	[32,06–34,06]	33,02
3	[13,82–14,71]	14,26	[35,13–36,09]	35,64
4	[14,92–16,22]	15,48	[37,02–38,9]	37,85
5	[16,41–17,66]	16,96	[40,07–41,14]	40,49
6	[17,77–19,0]	18,32	[41,65–43,82]	42,67
7	[19,34–20,29]	19,70	[43,87–46,24]	45,33
8	[20,58–21,24]	20,76	[45,56–48,52]	47,33
9	22,13	22,13	[48,71–51,08]	49,70
10	24,85	24,85	[51,89–53,52]	52,60

which makes this reference less reliable. Variations in water concentration can lead to disparate values for samples with the same fat content, complicating comparisons between them [4]. In fact, the chemical analyses carried out in the context of this study revealed the existence of these cases, as Fig. 5 illustrates by facing  $\overline{FCFW}_i$  values against those of  $\overline{FCDM}_i$ , for the 110 samples chemically analysed; certainly, FCDM only explains 72% of variance in FCFW. Considering this, the higher

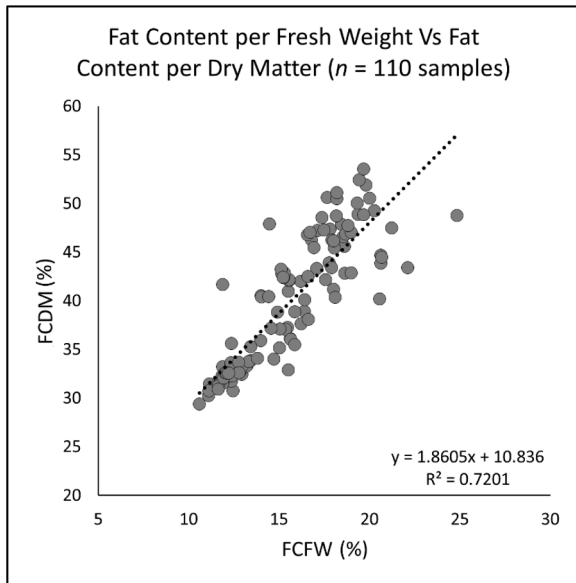


Fig. 5. Correlation study between fat content per fresh weight (FCFW) and fat content per dry matter (FCDM) values, for the 110 original fruit sets,  $\bar{F}_i$ , as determined by reference chemical analysis.

correlation observed with *FCDM* further strengthens confidence in capacitance measurement as an indicator of olive fat content, regardless of moisture variation. Conversely, it is reasonable to assume that water content plays a significant role in conductivity, a factor not addressed in the study by Justicia et al. [29], as previously mentioned.

The correlation analysis shown in Fig. 4 – (a-3) and (b-3), corroborates the previous findings and discussion. Notably, when clustering by percentiles, the correlation between the average electrical capacitance values for the 10 fruit sets,  $\bar{F}_{i,10}$ , and the corresponding *FCDM* reference values,  $\overline{FCDM}_{i,10}$ , even increases to 0,9741. In addition, the slope and intercept values of the resulting regression line are comparable to those previously obtained by grouping *FCDM* into 22 clusters. This result strengthens the hypothesis that considerable intra-sample variability existed in the original fruit sets, and supports the proposed methodology as a promising preliminary approach for assessing fat content in individual olive fruit samples.

Table 4 presents the Root-Mean-Square-Error values relative to the mean calculated from the actual fat content values and those estimated using the regression lines shown in Fig. 4. The metric was applied to the original *FCFW* and *FCDM* sets, and for those derived from clustering. Regarding *FCFW*, percentual error shows in general modest estimation performance for all the cases. For *FCFW*, the percentage error indicates modest estimation accuracy across all scenarios. Additionally, the error does not decrease with successive clustering, suggesting that water content variability inherent to *FCFW* significantly hinders the modelling of fat content based on capacitance measures. Conversely, average error values for *FCDM*, exhibit a clear downward trend, starting at 12,39% for the original dataset and reducing to an outstanding 2,66% for the decile-clustered subset. This pattern aligns with previous discussions,

Table 4

Values of Root-Mean-Square-Error (RMSE) relative to the mean calculated from the actual fat content values and those estimated using the regression lines shown in Fig. 4. Calculations were performed for the original *FCFW* and *FCDM* sets, and for those derived from clustering.

	$(\{FCFW_i\}, \{FCFW_i\})$	$(\{FCFW_{i,22}\}, \{FCFW_{i,22}\})$	$(\{FCFW_{i,10}\}, \{FCFW_{i,10}\})$
$RMSF_{mean}^{FCFW}$	15,69%	9,67%	13,86%
	$(\{FCDM_i\}, \{FCDM_i\})$	$(\{FCDM_{i,22}\}, \{FCDM_{i,22}\})$	$(\{FCDM_{i,10}\}, \{FCDM_{i,10}\})$
$RMSF_{mean}^{FCDM}$	12,39%	4,88%	2,66%

Table 5

Results of T-test for comparing the means of the pairs of equivalent reference and predicted distributions of *FCFW* and *FCDM*. Predicted distributions were obtained by applying the regression lines shown in Fig. 4. The results of Levene's test for equality of variances are also given.

	Levene's test ( $p < 0, 05$ )	T-test ( $p < 0, 05$ )		
		<i>t</i>	<i>p</i>	CI (95%)
$\{FCFW_i\}$ vs $\{FCFW_i\}$	$p = 0, 0^*$	0,011	0,992	[-0,65, 0,5]
$\{FCFW_{i,22}\}$ vs $\{FCFW_{i,22}\}$	$p = 0, 55$	-0,004	0,997	[-1,73, 1,72]
$\{FCFW_{i,10}\}$ vs $\{FCFW_{i,10}\}$	$p = 0, 388$	0,002	0,998	[-3,63, 3,63]
$\{FCDM_i\}$ vs $\{FCDM_i\}$	$p = 0, 0^*$	-0,004	0,997	[-1,49, 1,48]
$\{FCDM_{i,22}\}$ vs $\{FCDM_{i,22}\}$	$p = 0, 733$	-0,001	0,999	[-3,99, 3,99]
$\{FCDM_{i,10}\}$ vs $\{FCDM_{i,10}\}$	$p = 0, 920$	0,011	0,992	[-6,71, 6,78]

\* Welch's T-test [35] is used as significant differences in the variances of the samples are found.

reinforcing the hypothesis that the intra-sample variability present in the original fruit set is effectively captured and accounted for in the clustered datasets.

Table 5 presents the results of the T-test ( $p < 0, 05$ ) [35] conducted on the pairs of equivalent reference and predicted distributions of *FCFW* and *FCDM*. Notably, no significant differences were observed in the means of the reference and predicted sets in any case. However, the *p*-values from Levene's test [36] for equality of variances reveal trends consistent with those previously discussed and found with the other considered analyses. In the case of the original *FCFW* set, significant differences in variance were identified, whereas no significant differences were found in the clustered sets. Modest and non-systematic improvements in variance equality were observed as clustering progressed. For *FCDM*, significant differences in variance were also evident in the original dataset. Nevertheless, the *p*-value systematically and remarkably increased with clustering, reaching as high as 0,920 for the decile-clustered set. This trend highlights how the clustered sets were able to progressively represent intra-sample variability, revealing capacitance as a reliable indicator of *FCDM*.

#### 4. Conclusion

This paper presents a study examining how olive fruit maturation influences its capacity to store electrical charge. To this end, a custom-designed device was employed to measure the electrical capacitance of olive samples over the course of a full ripening season. These capacitance measurements were statistically compared with reference fat content values obtained through chemical analysis to evaluate their correlation. The results revealed strong correlation values with fat content per dry matter, particularly after accounting for and validating significant intra-sample variability. This finding aligns with recent studies suggesting that traditional ripeness assessments based on

external fruit appearance may not reliably indicate maturation stages. In contrast, the correlation with fat content per fresh weight was notably weaker, reinforcing the potential of capacitance as an indicator of olive fat content, irrespective of moisture variation. This behaviour was corroborated by applying the obtained regression lines to capacitance measurements to yield fat content estimates, and by analysing the precision and statistical coherence of the distributions of the estimated values.

From a scientific perspective, the presented device and methodology may serve as a valuable tool for studying olive fruit ripening variability with higher resolution. From a practical side, this approach could help olive growers sample their orchards easily, efficiently, and cost-effectively, allowing them to monitor fruit maturation throughout the season. Future research will focus on assessing the applicability of this methodology across different olive varieties, exploring ripening variability, and further refining and optimising the device's usability. In this regard, the potential impact of environmental condition variations on the accuracy of the developed meter is a significant concern, as it could constrain its applicability for directly characterising olive fat content under field conditions. Future research will focus on addressing this potential limitation.

### Ethics statement

Not applicable: This manuscript does not include human or animal research.

### CRedit authorship contribution statement

**Daniel Argüello:** Writing – review & editing, Writing – original draft, Investigation, Formal analysis, Data curation. **Miguel Noguera:** Writing – review & editing, Writing – original draft, Validation, Methodology, Investigation, Formal analysis, Data curation, Conceptualization. **Andrés Mejías:** Writing – review & editing, Writing – original draft, Methodology, Investigation, Formal analysis, Data curation, Conceptualization. **Juan Manuel Enrique:** Writing – review & editing, Writing – original draft, Validation, Methodology, Investigation, Formal analysis, Data curation, Conceptualization. **Arturo Aquino:** Writing – review & editing, Writing – original draft, Validation, Supervision, Resources, Project administration, Methodology, Investigation, Funding acquisition, Formal analysis, Data curation, Conceptualization.

### Declaration of competing interest

The authors declare that they have no known competing financial interests or personal relationships that could have appeared to influence the work reported in this paper.

### Funding

This work was supported by the Cooperation Program VI-A SPAIN-PORTUGAL (POCTEP) 2021–2027 and co-financed with ERDF [0067\_OLIVAR\_IA\_5\_E]; The Research Consolidation Programme 2022 of the Ministry of Science and Innovation (Spain) [CNS2022–136137]; and the Andalusian Plan for Research, Development and Innovation, PAIDI (Andalusia, Spain) [P18-RTJ-4539].

### Data availability

Data will be made available on request.

### References

- [1] FAOSTAT, (2024). <https://www.fao.org/faostat/en/#home> (accessed July 24, 2024).
- [2] R. Ghanbari, F. Anwar, K.M. Alkharfi, A.H. Gilani, N. Saari, Valuable Nutrients and Functional Bioactives in Different Parts of Olive (*Olea europaea* L.)—A Review, *Int. J. Mol. Sci.* 13 (2012) 3291–3340, <https://doi.org/10.3390/IJMS13033291>, 2012, Vol. 13, Pages 3291–3340.
- [3] R. Saullé, G. La Torre, The Mediterranean Diet, recognized by UNESCO as a cultural heritage of humanity, *Ital. J. Public Health.* 7 (2010) 414–415, <https://doi.org/10.2427/5700>.
- [4] L. Barranco Navero, Diego, Fernandez Escobar, Ricardo, Rallo Romero, El cultivo Del Olivo, 7a ed, Mundi-Prensa Libros, Madrid, 2017.
- [5] D.J. Connor, M. Gómez-del-Campo, M.C. Rousseaux, P.S. Searles, Structure, management and productivity of hedgerow olive orchards: A review, *Sci. Hortic. (Amsterdam)*. 169 (2014) 71–93, <https://doi.org/10.1016/J.SCIEN.2014.02.010>.
- [6] S. Fountas, K. Aggelopoulou, T.A. Gemtos, Precision agriculture: Crop management for improved productivity and reduced environmental impact or improved sustainability, in: D.A. Eleftherios Iakovou, Dionysis Bochtis, Dimitrios Vlachos (Eds.), *Supply Chain Manag. Sustain. Food Networks*, John Wiley & Sons, Ltd, 2015, pp. 41–65, <https://doi.org/10.1002/9781118937495.ch2>.
- [7] M. Hermoso, M. Uceda, A. García-Ortiz, J. Morales, L. Frías, A. Fernández, *Elaboración de aceite de oliva de calidad, Colección Apunt 5 (1991) 91*.
- [8] Asociación Española de Normalización y Certificación, UNE 55030:1961, Determination of the content in total fat of olives, España, 1961. <https://www.une.org/encuentra-tu-norma/busca-tu-norma/norma?c=N0005670> (accessed May 3, 2023).
- [9] A. Nordon, C.A. McGill, D. Littlejohn, Process NMR spectrometry, *Analyst* 126 (2001) 260–272, <https://doi.org/10.1039/B009293M>.
- [10] F. Grilo, T. Caruso, S.C. Wang, Influence of fruit canopy position and maturity on yield determinants and chemical composition of virgin olive oil, *J. Sci. Food Agric.* 99 (2019) 4319–4330, <https://doi.org/10.1002/JSSA.9665>.
- [11] J.M. Ponce, A. Aquino, B. Millan, J.M. Andujar, Automatic Counting and Individual Size and Mass Estimation of Olive-Fruits Through Computer Vision Techniques, *IEEE Access* 7 (2019) 59451–59465, <https://doi.org/10.1109/ACCESS.2019.2915169>.
- [12] W.H. Su, D.W. Sun, Multispectral Imaging for Plant Food Quality Analysis and Visualization, *Compr. Rev. Food Sci. Food Saf.* 17 (2018) 220–239, <https://doi.org/10.1111/1541-4337.12317>.
- [13] A.A. Gowen, C.P. O'Donnell, P.J. Cullen, G. Downey, J.M. Frias, Hyperspectral imaging – an emerging process analytical tool for food quality and safety control, *Trends Food Sci. Technol.* 18 (2007) 590–598, <https://doi.org/10.1016/J.TIFS.2007.06.001>.
- [14] A. Loutfi, S. Coradeschi, G.K. Mani, P. Shankar, J.B.B. Rayappan, Electronic noses for food quality: A review, *J. Food Eng.* 144 (2015) 103–111, <https://doi.org/10.1016/J.JFOODENG.2014.07.019>.
- [15] T.S. Awad, H.A. Moharram, O.E. Shaltout, D. Asker, M.M. Youssef, Applications of ultrasound in analysis, processing and quality control of food: A review, *Food Res. Int.* 48 (2012) 410–427, <https://doi.org/10.1016/J.FOODRES.2012.05.004>.
- [16] S.N. Jha, K. Narsaiah, A.L. Basediya, R. Sharma, P. Jaiswal, R. Kumar, R. Bhardwaj, Measurement techniques and application of electrical properties for nondestructive quality evaluation of foods—a review, *J. Food Sci. Technol.* 48 (2011) 387–411, <https://doi.org/10.1007/S13197-011-0263-X/TABLES/8>.
- [17] G.M. Weaver, H.O. Jackson, Electric impedance, an objective index of maturity in peach, *Can. J. Plant Sci.* 46 (1966) 323–326.
- [18] A. Alwis, F. Mitchell, Electrical conductivity meter for food samples, *IOPscience* 22 (1989) 554–556.
- [19] S.O. Nelson, Dielectric Properties of Agricultural Products: Measurements and Applications, *IEEE Trans. Electr. Insul.* 26 (1991) 845–869, <https://doi.org/10.1109/14.99097>.
- [20] F.R. Harker, J.H. Maindonald, Ripening of Nectarine Fruit (Changes in the Cell Wall, Vacuole, and Membranes Detected Using Electrical Impedance Measurements), *Plant Physiol* 106 (1994) 165–171, <https://doi.org/10.1104/PP.106.1.165>.
- [21] F.R. Harker, S.K. Forbes, Ripening and development of chilling injury in persimmon fruit: An electrical impedance study, *New Zeal. J. Crop Hortic. Sci.* 25 (1997) 149–157, <https://doi.org/10.1080/01140671.1997.9514001>.
- [22] A.R. Varlan, W. Sansen, Nondestructive Electrical Impedance Analysis in Fruit: Normal Ripening and Injuries Characterization, *Electro- and Magnetobiology* 15 (1996) 213–227, <https://doi.org/10.3109/15368379609012878>.
- [23] G.P. Sharma, S. Prasad, Dielectric properties of garlic (*Allium sativum* L.) at 2450 MHz as function of temperature and moisture content, *J. Food Eng.* 52 (2002) 343–348, [https://doi.org/10.1016/S0260-8774\(01\)00125-X](https://doi.org/10.1016/S0260-8774(01)00125-X).
- [24] M. Rehman, B.A.J.A. Abu Izneid, M.Z. Abdullah, M.R. Arshad, Assessment of quality of fruits using impedance spectroscopy, *Int. J. Food Sci. Technol.* 46 (2011) 1303–1309, <https://doi.org/10.1111/J.1365-2621.2011.02636.X>.
- [25] H. Cortes, V. Edgar, R. Suárez, J. Castillo, L.M. Gonçalves, P.R. Bueno, Pitahaya Aging Diagnostic by Impedance/Capacitance Spectroscopy, *Food Anal. Methods* 8 (2015) 126–129, <https://doi.org/10.1007/S12161-014-9878-7/TABLES/1>.
- [26] N. Nakawajana, A. Terdwongworakul, S. Teerachaichayut, Minimally destructive assessment of mangosteen translucency based on electrical impedance measurements, *J. Food Eng.* 171 (2016) 137–144, <https://doi.org/10.1016/J.JFOODENG.2015.10.020>.
- [27] H. Lan, Z. Wang, H. Niu, H. Zhang, Y. Zhang, Y. Tang, Y. Liu, A nondestructive testing method for soluble solid content in Korla fragrant pears based on electrical properties and artificial neural network, *Food Sci. Nutr.* 8 (2020) 5172–5181, <https://doi.org/10.1002/fsn3.1822>.
- [28] M. Mohammed, M. Munir, A. Aljabr, Prediction of Date Fruit Quality Attributes during Cold Storage Based on Their Electrical Properties Using Artificial Neural Networks Models, *Foods* 11 (2022) 1666, <https://doi.org/10.3390/FOODS11111666>, 2022, Vol. 11, Page 1666.

- [29] M. Justicia, A. Madueño, A. Ruiz-Canales, J.M. Molina, M. López, J.M. Madueño, J. A. Granados, Low-frequency characterisation of mesocarp electrical conductivity in different varieties of olives (*Olea europaea* L.), *Comput. Electron. Agric.* 142 (2017) 338–347, <https://doi.org/10.1016/j.compag.2017.09.021>.
- [30] W. Köppen, R. Geiger, *Handbuch Der Klimatologie: Das Geographische System der Klimate*, 1st ed, Gebrüder Borntraeger, Berlin, 1936.
- [31] J. Ferreira, *Explotaciones oliveras colaboradoras*, 1979.
- [32] International Organization of Standardization. ISO 662:2016., *Animal and vegetable fats and oils - Determination of moisture and volatile matter content*, España, 2016. <https://www.une.org/encuentra-tu-norma/busca-tu-norma/norma/?c=norma-une-en-iso-662-2001-n0025256> (accessed May 3, 2023).
- [33] Capacitor | Arduino Documentation. <https://docs.arduino.cc/libraries/capacitor/> (accessed November 12, 2024).
- [34] MKR Zero | Arduino Documentation. <https://docs.arduino.cc/hardware/mkr-zero/> (accessed November 12, 2024).
- [35] A. Field, *Discovering Statistics Using IBM SPSS Statistics*, 4th ed., SAGE Publications, London, 2013.
- [36] H. Levene, Robust tests for equality of variances, in: I. Olkin, S.G. Ghurye, W. Hoeffding, W.G. Madow, H.B. Mann (Eds.), *Contributions to Probability and Statistics. Essays in Honor of Harold Hotelling*, Stanford University Press, Stanford, California, 1961, pp. 279–292.